CHAPTER 10

MULTIAXIAL STRESSES

Multiaxial states of stress are very common, and multiaxial strain is difficult to avoid. The strains are triaxial, for example, in a tensile bar. With longitudinal strain ε we have two transverse strains $-\nu\varepsilon$, where ν is Poisson's ratio, which changes from about 0.3 in the elastic range to 0.5 in the plastic range. In a shaft that transmits torque, there are two principal stresses σ, equal in magnitude but opposite in sign. There is neither stress nor strain in the third principal direction. In a thin-walled pressure vessel subjected to cyclic pressure, the longitudinal and hoop stresses are also principal stresses whose directions remain fixed during pressure cycling. In a crankshaft we have torsion and bending. On points of its surface, two principal stresses exist that vary in magnitude and direction. The frequencies of the bending cycles and torsion cycles are not the same. Most points on the surface have triaxial strain. The state of stress in notches is usually multiaxial and is not the same as the state of stress in the main body. For example, at the root of a thread the state of stress is biaxial, although it may be uniaxial in the main body of a bolt. In addition, the stress concentration factor changes with the state of stress, and stress and strain concentration factors are not equal.

Can we somehow manage to apply our knowledge and data from uniaxial behavior and tests to multiaxial situations? This is the question with which this chapter is concerned. We first briefly review states of stress and strain and classify constant amplitude multiaxial loading into proportional and nonproportional loading. This is followed by a brief discussion of yielding and plasticity under multiaxial stress states. Multiaxial fatigue life estimation methods are then classified and described as stress-based approaches, strain-based and energy-based approaches including critical plane models, and the fracture

mechanics approach for crack growth. In these discussions we assume isotropic material, although it is known that the fatigue properties of some materials may not be isotropic; for example, the fatigue strength in the direction of rolling or extruding may be substantially greater than that in the transverse direction. Also, unnotched behavior and constant amplitude loading are emphasized, while brief discussions of notched effects and variable amplitude loading are included at the end of the chapter.

10.1 STATES OF STRESS AND STRAIN AND PROPORTIONAL VERSUS NONPROPORTIONAL LOADING

An understanding of the state of stress and strain in a component or structure is essential for multiaxial fatigue analysis. The state of stress and strain at a point in the body can be described by six stress components (σ_x, σ_y, σ_z, τ_{xy}, τ_{xz}, τ_{yz}) and six strain components (ε_x, ε_y, ε_z, γ_{xy}, γ_{xz}, γ_{yz}) acting on orthogonal planes x, y, and z. Stresses and strains acting in any other direction or plane can be found by using transformation equations or graphically by using Mohr's circle.

Of special interest to fatigue analysis are the magnitudes and directions of the maximum normal principal stress, σ_1, the maximum shearing stress, $\tau_{\max}$, the maximum normal principal strain, ε_1, and the maximum shearing strain, $\gamma_{\max}$, acting at a critical location in the component or structure. It is important to realize that even though only a few planes experience the maximum principal normal stress (or strain) and the maximum shearing stress (or strain), many other planes can experience a very large percentage of these quantities. For example, with simple uniaxial tension, even though only the loading plane experiences the maximum normal stress σ_1, all planes oriented between $\pm 13°$ from the loading plane experience at least 95 percent of σ_1. Also, a shearing stress is present on every stressed plane, except for the loading plane. In addition to the maximum principal stress or strain plane and the maximum shear planes, the octahedral planes are of importance in yielding prediction and fatigue analysis. There are eight octahedral planes making equal angles with the three principal stress directions. The shearing stress on these planes is given by

$$\tau_{\text{oct}} = \frac{1}{3}\sqrt{(\sigma_1 - \sigma_2)^2 + (\sigma_2 - \sigma_3)^2 + (\sigma_3 - \sigma_1)^2} \tag{10.1}$$

The normal stress on an octahedral plane is the hydrostatic stress (also called the "average normal stress") given by

$$\sigma_{\text{oct}} = \sigma_h = \sigma_{\text{ave}} = \frac{1}{3}(\sigma_1 + \sigma_2 + \sigma_3) \tag{10.2}$$

The shear strain acting on an octahedral plane is given by

$$\gamma_{oct} = \frac{2}{3}\sqrt{(\varepsilon_1 - \varepsilon_2)^2 + (\varepsilon_2 - \varepsilon_3)^2 + (\varepsilon_3 - \varepsilon_1)^2} \qquad (10.3)$$

During constant amplitude cyclic loading, as the magnitudes of the applied stresses vary with time, the size of Mohr's circle of stress also varies with time. In some cases, even though the size of Mohr's circle varies during cyclic loading, the orientation of the principal axes with respect to the loading axes remains fixed. This is called "proportional loading." In many cases, however, the principal directions of the alternating stresses are not fixed in the stressed part but change orientation. Crankshafts are a typical example. Shafts subjected to out-of-phase torsion and bending are another. This type of loading is called "nonproportional loading." Proportional and nonproportioinal loading are illustrated by Fig. 10.1 for combined axial-torsion loading of a shaft shown in Fig. 10.1*a*. The loads in Fig. 10.1*b* are applied in-phase, so that the maximum and minimum axial and torsion stresses occur simultaneously. The ratio of axial stress, σ_y, and torsion stress, τ_{xy}, remains constant during cycling, as shown by the linear relationship in Fig. 10.1*c*. This is therefore called "proportional loading." If the loads are applied 90° out-of-phase (Fig. 10.1*d*), the stress path, σ_y–τ_{xy}, follows an ellipse, as shown in Fig. 10.1*c*. The ratio of axial stress, σ_y, and torsion stress, τ_{xy}, varies continuously during the cycle. This is therefore an example of nonproportional loading. Mohr's circles of stress at times 2 and 3 during the in-phase loading cycle are shown in Fig. 10.1*e*. It can be seen that the orientation of the principal normal stress directions remains fixed (i.e., angle 2α remains constant), even though the size of the circle changes as the magnitudes of the loads vary with time. Mohr's circles of stress at three times (1, 2, and 3) during the out-of-phase loading cycle are shown in Fig. 10.1*f*. For this case, the orientations of the principal normal stress axes rotate continuously with respect to the loading axes (i.e., x–y axes). The maximum principal normal stress axis orientation starts out at $\alpha = 45°$ at time 1, decreases to a smaller α at time 2, and rotates to $\alpha = 0°$ at time 3. Then it continues to rotate in a clockwise direction until point 9, where it returns to $\alpha = 45°$.

10.2 YIELDING AND PLASTICITY IN MULTIAXIAL FATIGUE

As discussed in Chapter 3, cyclic plastic deformation is an essential component of the fatigue damage process. Therefore, an understanding of multiaxial cyclic plastic deformation is often necessary, particularly in situations where significant plasticity exists, such as at notches and in low-cycle fatigue. The basic elements of plasticity theory consist of a yield function to determine when plastic flow begins, a flow rule which relates the applied stress increments

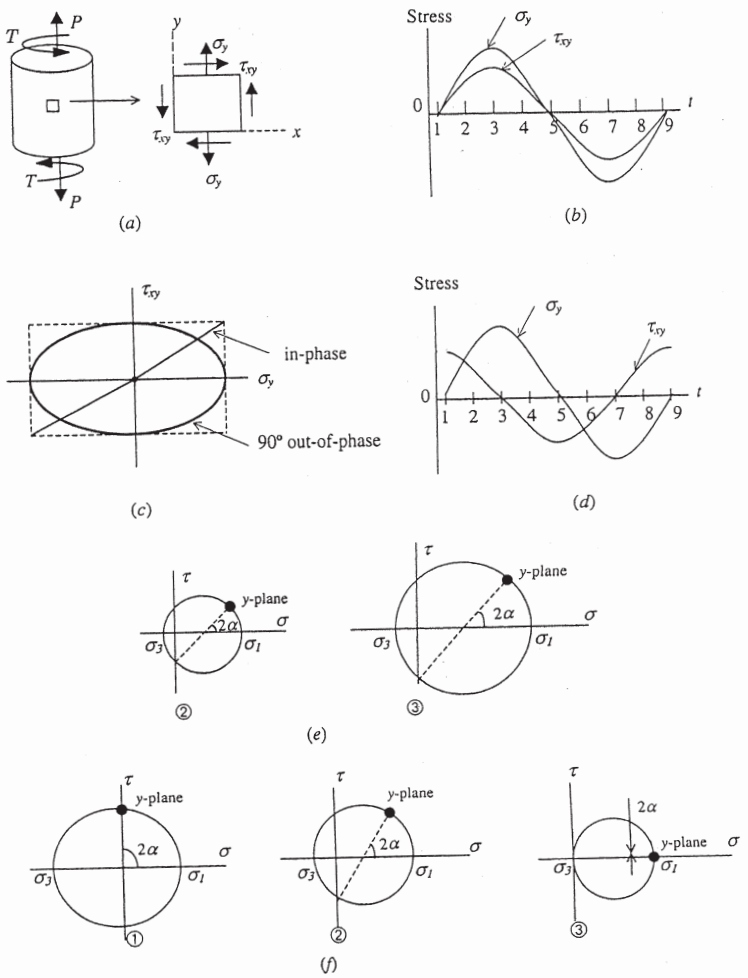

Figure 10.1 Illustration of proportional or in-phase and nonproportional or 90° out-of-phase loading. (*a*) Stress element in axial-torsion loading. (*b*) Applied in-phase axial and shear stress histories. (*c*) Stress path for in-phase and 90° out-of-phase loading. (*d*) Applied 90° out-of-phase axial and shear stress histories. (*e*) Mohr's circle of stress at times 2 and 3 in the cycle for in-phase loading. (*f*) Mohr's circle of stress at times 1, 2, and 3 in the cycle for 90° out-of-phase loading.

to the resulting plastic strain increments once plastic flow has begun, and a hardening rule that describes the change in the yield criterion as a function of plastic strains. Time effects such as creep and viscoelasticity are neglected here, so that yielding depends only on instantaneous increments of stress or strain and on the previous history of the material.

The yield criterion can be visualized in a "stress space" in which each of the coordinate axes represents one principal stress. A commonly used yield criterion for metals is the von Mises yield criterion, which can be visualized as a circular cylinder in the stress space. For unyielded material the axis of the cylinder passes through the origin of the coordinates. It is inclined equal amounts to the three coordinate axes and represents pure hydrostatic stress (i.e., $\sigma_1 = \sigma_2 = \sigma_3$). The von Mises yield criterion is given by

$$\sqrt{(\sigma_1 - \sigma_2)^2 + (\sigma_2 - \sigma_3)^2 + (\sigma_3 - \sigma_1)^2} = 2S_y^2 \tag{10.4}$$

where S_y is the material yield strength. For biaxial or plane states of stress ($\sigma_3 = 0$), the yield condition is the intersection of the cylinder with the σ_1–σ_2 plane, which is a yield ellipse.

It is often convenient to convert the multiaxial stress state to an "equivalent" stress, σ_e, which is the uniaxial stress that is equally distant from (or located on) the yield surface. During initial loading, the von Mises equivalent stress is given by

$$\sigma_e = \frac{1}{\sqrt{2}}\sqrt{(\sigma_1 - \sigma_2)^2 + (\sigma_2 - \sigma_3)^2 + (\sigma_3 - \sigma_1)^2} \tag{10.5}$$

or

$$\sigma_e = \frac{1}{\sqrt{2}}\sqrt{(\sigma_x - \sigma_y)^2 + (\sigma_y - \sigma_z)^2 + (\sigma_z - \sigma_x)^2 + 6\,(\tau_{xy}^2 + \tau_{yz}^2 + \tau_{zx}^2)} \tag{10.6}$$

where σ_x, τ_{xy}, and so on are stresses in an arbitrary orthogonal coordinate system. Yielding occurs when $\sigma_e = S_y$. These expressions for the equivalent stress, σ_e, are also related to the octahedral shear stress and the distortion energy.

Once plastic deformation has begun, we need a flow rule to relate stresses and plastic strains. Equations relating stresses and plastic strains are also called "constitutive equations" and are typically based on the normality condition. This condition states that the increment of plastic strain caused by an increment of stress is such that the vector representing the plastic strain increment is normal to the yield surface during plastic deformation.

A hardening rule is needed to describe the behavior of the material once it is plastically deformed or yielded. One possible hardening rule is the isotropic rule, which assumes that strain hardening corresponds to an enlargement of

the yield surface (i.e., an increase in S_y) without a change of shape or position in the stress space. Another is the kinematic rule, which assumes that strain hardening shifts the yield surface without changing its size or shape. A version of the kinematic hardening rule commonly used in cyclic plasticity is the Mroz kinematic hardening rule.

Nonproportional multiaxial cyclic loading often produces additional strain hardening which is not observed under proportional loading conditions. Therefore, the cyclic stress–strain curve for nonproportional loading is above that for proportional loading. The reason for the additional hardening is the interaction of slip planes, since many more slip planes are active during nonproportional loading due to the rotation of the principal axes, as discussed in Section 10.1. The amount of this additional hardening depends on the degree of load nonproportionality as well as on the material. Models to incorporate this additional hardening are discussed in [1].

10.3 STRESS-BASED CRITERIA

10.3.1 Equivalent Stress Approaches

Equivalent stress approaches are extensions of static yield criteria to fatigue. The most commonly used equivalent stress approaches for fatigue are the maximum principal stress theory, the maximum shear stress theory (also called Tresca theory), and the octahedral shear stress theory (or von Mises theory). An "equivalent" nominal stress amplitude, S_{qa}, can be computed according to each criterion as

Maximum principal stress theory:
$$S_{qa} = S_{a1} \tag{10.7}$$

Maximum shear stress theory:
$$S_{qa} = S_{a1} - S_{a3} \tag{10.8}$$

Octahedral shear stress theory:
$$S_{qa} = \frac{1}{\sqrt{2}}\sqrt{(S_{a1} - S_{a2})^2 + (S_{a2} - S_{a3})^2 + (S_{a3} - S_{a1})^2} \tag{10.9}$$

Here S_{a1}, S_{a2}, and S_{a3} are principal alternating nominal stresses with $S_{a1} > S_{a2} > S_{a3}$. Note that Eq. 10.9 is identical to Eq. 10.5 for von Mises equivalent stress for static loading, except that alternating stresses are used. This criterion can also be written in terms of the x, y, z stress components, with the resulting equation identical to Eq. 10.6 but with alternating stresses. Once the equivalent nominal stress amplitude, S_{qa}, is calculated, the multiaxial stress state is reduced to an equivalent uniaxial stress state. Therefore, the S–N approach discussed in Chapter 4 can then be used for fatigue life calculations by setting S_{qa} equal to the appropriate fatigue strength S_{Nf} or S_f.

The octahedral shear stress criterion (von Mises) is the most widely used equivalent stress criterion for multiaxial fatigue of materials having ductile

behavior. The maximum principal stress criterion is usually better for multiaxial fatigue of materials having brittle behavior. The three aforementioned criteria are shown in Fig. 10.2 for biaxial stress states ($S_3 = 0$) [2]. The coordinate axes in this figure are the principal alternating stresses (S_{a1} and S_{a2}), normalized by the uniaxial fatigue strength, S_f. Multiaxial in-phase fatigue data at long lives (10^7 cycles) for different combinations of fully reversed alternating stresses for a mild steel, a chromium–vanadium (Cr–V) steel, and a cast iron are also plotted in Fig. 10.2. It can be seen that data for the mild steel and Cr–V steel, which behave in a ductile manner, agree well with the octahedral shear stress criterion. The data for cast iron, which behaves in a brittle manner, agree better with the maximum principal stress criterion.

If mean or residual stresses are present, an equivalent mean nominal stress, S_{qm}, can be calculated based on the von Mises effective stress:

$$S_{qm} = \frac{1}{\sqrt{2}} \sqrt{(S_{m1} - S_{m2})^2 + (S_{m2} - S_{m3})^2 + (S_{m3} - S_{m1})^2} \quad (10.10)$$

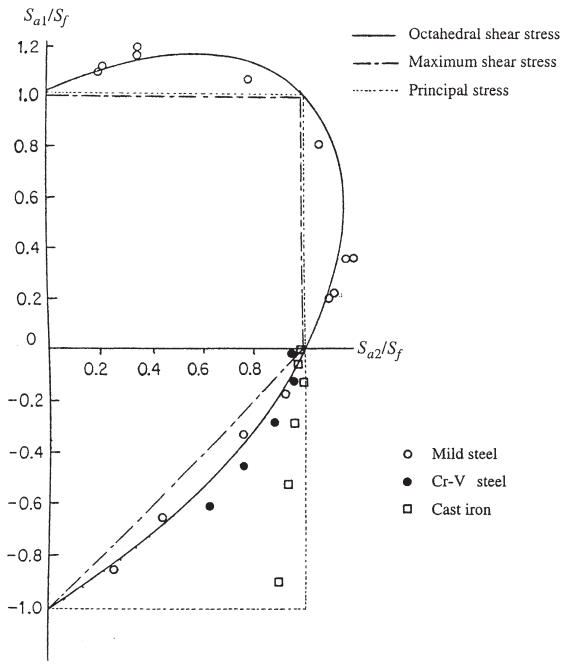

Figure 10.2 Comparison of biaxial fatigue data with equivalent stress failure criteria [2].

where S_{m1}, S_{m2}, and S_{m3} are principal mean nominal stresses. Another commonly used equivalent mean stress is the sum of mean normal stresses:

$$S_{qm} = S_{m1} + S_{m2} + S_{m3} = S_{mx} + S_{my} + S_{mz} \quad (10.11)$$

Note that the second equality in Eq. 10.11 exists because the sum of normal stresses represents a stress invariant (i.e., a stress quantity independent of the coordinate axes used). Both the Tresca and von Mises equivalent stresses are insensitive to a hydrostatic stress (i.e., $S_{m1} = S_{m2} = S_{m3}$). Therefore, if the mean stress is hydrostatic, Eq. 10.10 results in $S_{qm} = 0$. Since fatigue life has been observed to be sensitive to hydrostatic stress, the use of Eq. 10.11 is preferred for this case. In addition, Eq. 10.10 always results in a positive equivalent mean stress, whereas Eq. 10.11 can be either positive or negative. Equation 10.11, therefore, better represents the beneficial effect of compressive mean stress and the detrimental effect of tensile mean stress on fatigue life. Also, according to Eq. 10.11, mean torsion stress has no direct influence on fatigue (i.e., $S_{qm} = 0$ for mean torsion). This agrees with experimental evidence, as long as the maximum shear stress remains below yielding for the material. If the maximum shear stress is high enough to produce yielding, it may change residual stresses and indirectly affect fatigue resistance. This equation, however, suggests that the effect of a tensile mean stress acting in one direction can be nullified by a compressive mean stress acting in another direction (e.g., in plane stress $S_{qm} = 0$ if $S_{mx} = -S_{my}$), which does not necessarily agree with experimental evidence.

Stresses S_{qa} and S_{qm} are those equivalent alternating and mean stresses that can be expected to give the same life in uniaxial loading as in multiaxial loading. After S_{qa} and S_{qm} are calculated, the expected fatigue life is found from the formulas for uniaxial fatigue, such as the modified Goodman equation (Eq. 4.8). The formulas are used with the magnitude of S_{qa} in place of S_a and with the magnitude of S_{qm} in place of S_m.

Equivalent stress approaches have been commonly used because of their simplicity, but their success in correlating multiaxial fatigue data has been limited to a few materials and loading conditions. In addition, they should be used only for proportional loading conditions, in which the principal axes directions remain fixed during the loading cycle.

10.3.2 Sines Method

Sines method [2] uses the alternating octahedral shear stress for cyclic stresses (i.e., Eq. 10.1 in terms of principal alternating nominal stresses) and the hydrostatic stress for mean stresses (i.e., Eq. 10.2 in terms of principal mean or residual nominal stresses). It can be represented by

$$\sqrt{(S_{a1} - S_{a2})^2 + (S_{a2} - S_{a3})^2 + (S_{a3} - S_{a1})^2} + m\,(S_{mx} + S_{my} + S_{mz}) = \sqrt{2}\,S_{Nf} \quad (10.12)$$

where m is the coefficient of mean stress influence and S_{Nf} is the uniaxial, fully reversed fatigue strength that is expected to give the same fatigue life on uniaxial smooth specimens as the multiaxial stress state. The coefficient m can be determined experimentally by obtaining a fatigue strength with a nonzero mean stress level (e.g., uniaxial fatigue strength for $R = 0$ condition where $S_m = S_a$). The value of m is on the order of 0.5. If plotted in terms of principal alternating stresses for biaxial stress states, the Sines method is similar to the octahedral shear stress theory shown in Fig. 10.2, except that the ellipse becomes smaller for a positive mean stress term and larger for a negative mean stress term. In terms of x, y, z stress components, the Sines method is expressed by the equation

$$\sqrt{(S_{ax} - S_{ay})^2 + (S_{ay} - S_{az})^2 + (S_{az} - S_{ax})^2 + 6\,(\tau_{axy}^2 + \tau_{ayz}^2 + \tau_{azx}^2)} + m\,(S_{mx} + S_{my} + S_{mz}) = \sqrt{2}\,S_{Nf} \quad (10.13)$$

The multiaxial stress state is then reduced to an equivalent uniaxial stress, S_{Nf}. The Sines method should also be limited to those cases in which the principal alternating stresses do not change their directions relative to the stressed part (i.e., proportional loading). For this type of loading, this theory fits most observations for long life fatigue and can be extended for application to strain-controlled, low-cycle fatigue.

10.3.3 Examples Using the Stress–Life Approach

We use two examples to illustrate applications of the S–N approach. Both examples involve proportional biaxial loading. As discussed in other chapters, it should be recognized that stress-based approaches are, in general, suitable for long life fatigue situations, in which strains are mainly elastic.

Example 1 A closed-end, thin-walled tube made of 1020 sheet steel, with inside diameter $d = 100$ mm (4 in.) and wall thickness $t = 3$ mm (0.12 in.), is subject to internal pressure, p, which fluctuates from 0 to 15 MPa (2.18 ksi). What is the expected fatigue life?

Stress analysis shows a longitudinal stress varying from 0 minimum to $pd/4t = (15 \times 100)/12 = 125$ MPa maximum and a circumferential stress varying from 0 to $pd/2t = 250$ MPa maximum, which is in-phase with, or proportional to, the longitudinal stress. These stresses are also the principal stresses such that $S_1 = 250$ MPa and $S_2 = 125$ MPa. The radial stress in a thin-walled tube is small compared to the longitudinal and circumferential stresses such that $S_3 \approx 0$.

For fatigue analysis we separate the stresses into alternating and mean components:

$$S_{a1} = S_{m1} = 125 \text{ MPa} \quad \text{and} \quad S_{a2} = S_{m2} = 62.5 \text{ MPa}$$

We then form "equivalent" alternating and mean stresses. They are equivalent because we expect their joint effect to give the same life in uniaxial tests that we expect from the multiaxial situation. The equivalent alternating stress is calculated from Eq. 10.9:

$$S_{qa} = \frac{1}{\sqrt{2}}\sqrt{(125 - 62.5)^2 + (62.5 - 0)^2 + (0 - 125)^2} = 108 \text{ MPa}$$

The equivalent mean stress from Eq. 10.11 is simply the sum of the mean normal stresses in three mutually perpendicular directions, $S_{qm} = 125 + 62.5 = 187.5$ MPa. With S_{qa} and S_{qm} values known, we can use the modified Goodman equation (Eq. 4.8) to obtain the uniaxial, fully reversed fatigue strength, S_{Nf}. From Table A.2 for 1020 HR sheet steel, $S_u = 441$ MPa. Then

$$\frac{S_{qa}}{S_{Nf}} + \frac{S_{qm}}{S_u} = \frac{108}{S_{Nf}} + \frac{187.5}{441} = 1 \quad \text{or} \quad S_{Nf} = 188 \text{ MPa}$$

Now the fatigue life can be calculated using Basquin's S–N equation with cyclic properties of the material from Table A.2

$$S_{Nf} = \sigma_f'(2N_f)^b = 1384\,(2N_f)^{-0.156}$$

Substituting $S_{Nf} = 188$ MPa results in $N_f = 180\,000$ cycles. If we use the Sines method with $m = 0.5$, Eq. 10.12 results in

$$\sqrt{(125 - 62.5)^2 + (62.5 - 0)^2 + (0 - 125)^2} + 0.5\,(125 + 62.5 + 0) = \sqrt{2}\,S_{Nf}$$

from which we obtain $S_{Nf} = 175$ MPa, resulting in $N_f = 290\,000$ cycles. The difference between the two results in less than a factor of 2.

Example 2 Consider a shaft with a diameter of 20 mm (0.8 in.) carrying a gear with a pitch diameter of 110 mm (4.33 in.) on its end. The tangential force on the gear is 8000 N (1800 lb), and the radial force is neglected. The distance from the center of the gear to a bearing is 25 mm (1 in.). How do we compare this stress situation to test data from uniaxial stresses?

The bending moment is $M = 8000 \times 0.025 = 200$ N.m and the torque is $T = 8000 \times 0.055 = 440$ N.m. Both bending stress, S, and torsion stress, τ, are found on the surface of the shaft at the bearing as follows:

$$S = 200\,\frac{32 \times 10^6}{\pi \times 2^3} \text{ Pa} = 255 \text{ MPa} \quad \text{and} \quad \tau = 440\,\frac{16 \times 10^6}{\pi \times 2^3} \text{ Pa} = 280 \text{ MPa}$$

The bending stress is fully reversed since the shaft rotates with $S_a = 255$ MPa, while the torsion stress is a steady stress with $\tau_m = 280$ MPa. We calculate S_{qa} from Eq. 10.9 with $S_{a1} = S_a = 255$ MPa and $S_{a2} = S_{a3} = 0$.

$$S_{qa} = \frac{1}{\sqrt{2}}\sqrt{(255 - 0)^2 + 0^2 + (0 - 255)^2} = 255 \text{ MPa}$$

According to Eq. 10.11, $S_{qm} = 280 - 280 = 0$, since principal stresses in torsion are equal to shear stress, $S_{m1} = \tau_m$, $S_{m2} = 0$, and $S_{m3} = -\tau_m$. The fatigue life of this shaft is, therefore, expected to be about that for uniaxial stressing (i.e., rotating bending) of the same shaft, with $S_a = S_{qa} = 255$ MPa and without the mean torque (i.e., $S_m = S_{qm} = 0$). The Sines method predicts the same result as the octahedral shear stress criterion, since the mean stress term in Eq. 10.12 is zero. In this example, the principal axes do not remain fixed on the shaft. However, the principal axes for the alternating stress components do not rotate with time. As a result, this loading can also be classified as proportional cyclic loading, and no additional strain hardening, as discussed in Section 10.2, is associated with this loading.

10.4 STRAIN-BASED, ENERGY-BASED, AND CRITICAL PLANE APPROACHES

10.4.1 Strain-Based and Energy-Based Approaches

Strain-based approaches are used with the strain–life curve (Eq. 5.14) in situations in which significant plastic deformation can exist, such as in low-cycle fatigue or at notches. Analogous to equivalent stress approaches, equivalent strain approaches have been used as strain-based multiaxial fatigue criteria. The most commonly used equivalent strain approaches are strain versions of the equivalent stress models discussed in Section 10.3.1 as follows:

Maximum principal strain theory:
$$\varepsilon_{qa} = \varepsilon_{a1} \tag{10.14}$$

Maximum shear strain theory:
$$\varepsilon_{qa} = \frac{\varepsilon_{a1} - \varepsilon_{a3}}{1 + \nu} \tag{10.15}$$

Octahedral shear strain theory:
$$\varepsilon_{qa} = \frac{\sqrt{(\varepsilon_{a1} - \varepsilon_{a2})^2 + (\varepsilon_{a2} - \varepsilon_{a3})^2 + (\varepsilon_{a3} - \varepsilon_{a1})^2}}{\sqrt{2}\,(1 + \nu)} \tag{10.16}$$

where ε_{a1}, ε_{a2}, and ε_{a3} are principal alternating strains with $\varepsilon_{a1} > \varepsilon_{a2} > \varepsilon_{a3}$. Once an equivalent alternating strain, ε_{qa}, has been calculated from the multiaxial stress state, the strain–life equation (Eq. 5.14 with ε_a replaced by ε_{qa}) is used for fatigue life prediction. Similar to the equivalent stress approaches, equivalent strain approaches are also not suitable for nonproportional multiaxial loading situations, in which the principal alternating strain axes rotate during cycling.

Energy-based approaches use products of stress and strain to quantify fatigue damage. Several energy quantities have been proposed for multiaxial fatigue, such as the plastic work per cycle as the parameter for life to crack nucleation. Plastic work is calculated by integrating the product of the stress and the plastic strain increment (the area of the hysteresis loop) for each of the six components of stress. The sum of the six integrals is the plastic work per cycle. The determination of the hysteresis loops σ_x–ε_x, τ_{xy}–γ_{xy}, and so on requires careful consideration of hardening rules and flow rules, particularly during nonproportional loading, since the shape of the hysteresis loops depends on the loading path. Application of this method to high-cycle fatigue situations is difficult since plastic strains are small. Models based on total strain energy density per cycle, consisting of both elastic and plastic energy density terms, have also been developed by Ellyin [3] and co-workers and by Park and Nelson [4]. Energy-based approaches can be used for nonproportional loading. Energy, however, is a scalar quantity and, therefore, does not reflect fatigue damage nucleation and growth observed on specific planes.

10.4.2 Critical Plane Approaches and the Fatemi-Socie Model

Experimental observations indicate that cracks nucleate and grow on specific planes (also called "critical planes"). Depending on the material and loading conditions, these planes are either maximum shear planes or maximum tensile stress planes. Multiaxial fatigue models relating fatigue damage to stresses and/or strains on these planes are called "critical plane models." These models, therefore, can predict not only the fatigue life, but also the orientation of the crack or failure plane. Different damage parameters using stress, strain, or energy quantities have been used to evaluate damage on the critical plane.

A critical plane model based on stress quantities was developed by Findley for high-cycle fatigue in the 1950s [5]. Findley identified the cyclic shear stress and the normal stress on the shear stress plane as the parameters governing fatigue damage. Findley's model can be described as

$$\frac{\Delta\tau}{2} + k\sigma_n = C \tag{10.17}$$

where $\Delta\tau/2$ is the shear stress amplitude, σ_n is the normal stress acting on the $\Delta\tau$ plane, and k and C are constants. According to this model, failure (as defined by crack nucleation and growth of small cracks) occurs on the plane with the largest value of $(\Delta\tau/2 + k\sigma_n)$. Later, Brown and Miller [6] formulated a similar approach in terms of strains, where the cyclic shear strain and the

normal strain on the maximum shear plane are the governing parameters. A simple formulation of this approach is given by

$$\frac{\Delta\gamma_{\max}}{2} + s\,\Delta\varepsilon_n = C \tag{10.18}$$

where $\Delta\gamma_{\max}/2$ is the maximum shear strain amplitude, $\Delta\varepsilon_n$ is the normal strain range on the $\Delta\gamma_{\max}$ plane, and s is a material dependent constant that weights the importance of normal strain for different materials.

Critical plane approaches attempt to reflect the physical nature of fatigue damage (i.e., damage mechanisms) in their formulation. A common model based on the physical interpretation of fatigue damage is the Fatemi-Socie model [7]. In this model, the parameters governing fatigue damage are the maximum shear strain amplitude, $\Delta\gamma_{\max}/2$, and the maximum normal stress, $\sigma_{n,\max}$, acting on the maximum shear strain amplitude plane. The physical basis for this model is illustrated in Fig. 10.3. Cracks are usually irregularly shaped at the microscopic level, as the crack grows through the material grain structure. This results in interlocking and friction forces between crack surfaces during cyclic shear loading (i.e., crack closure), as shown in Fig. 10.3*a*. Consequently, the crack tip driving force is reduced and the fatigue life is increased. A tensile stress perpendicular to the crack plane tends to separate crack surfaces, and therefore, reduce interlocking and frictional forces, as shown in Fig. 10.3*b*. This increases the crack tip driving force, and the fatigue life is reduced. Fractographic evidence of this behavior has been reported [8,9]. The Fatemi-Socie model is expressed as

$$\frac{\Delta\gamma_{\max}}{2}\left(1 + k\,\frac{\sigma_{n,\max}}{S_y}\right) = C \tag{10.19}$$

where S_y is the material monotonic yield strength and k is a material constant. The maximum normal stress is normalized by the yield strength to preserve

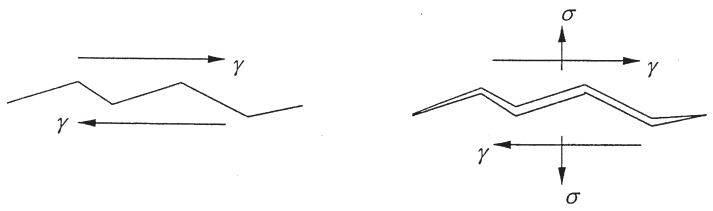

(*a*) (*b*)

Figure 10.3 Physical basis of the Fatemi-Socie model. (*a*) Shear loading of a crack. (*b*) Effect of tensile stress on the shear crack.

the unitless feature of strain. The value of k can be found by fitting fatigue data from simple uniaxial tests to fatigue data from simple torsion tests (note that for the simple torsion test, $\sigma_{n,\max} = 0$, and the left side of Eq. 10.19 reduces to $\Delta\gamma_{\max}/2$). As a first approximation or if test data are not available, $k \approx 1$.

Mean or residual stress effects on fatigue life in this model are accounted for by the maximum normal stress term, since

$$\sigma_{n,\max} = \sigma_{n,a} + \sigma_{n,m} \tag{10.20}$$

where $\sigma_{n,a}$ and $\sigma_{n,m}$ are the alternating normal and mean or residual normal stresses, respectively. Additional hardening resulting from nonproportional loading, as discussed in Section 10.2, is also incorporated by the maximum normal stress term since additional hardening results in an increase in the alternating normal stress, $\sigma_{n,a}$.

Equation 10.19 can be written in terms of shear strain–life properties obtained from fully reversed torsion tests (usually using thin-walled tube specimens) as

$$\frac{\Delta\gamma_{\max}}{2}\left(1 + k\,\frac{\sigma_{n,\max}}{S_y}\right) = \frac{\tau_f'}{G}(2N_f)^{b_0} + \gamma_f'\,(2N_f)^{c_0} \tag{10.21}$$

where G is the shear modulus, τ_f' is the shear fatigue strength coefficient, γ_f' is the shear fatigue ductility coefficient, and b_0 and c_0 are shear fatigue strength and shear fatigue ductility exponents, respectively. If these properties are not available, they can be estimated from uniaxial strain–life properties as $\tau_f' \approx \sigma_f'/\sqrt{3}$, $b_0 \approx b$, $\gamma_f' \approx \sqrt{3}\,\varepsilon_f'$, and $c_0 \approx c$. Equation 10.19 can also be expressed in terms of the uniaxial strain–life properties in Eq. 5.14 by equating the left side of Eq. 10.19 to C for fully reversed, uniaxial straining:

$$\frac{\Delta\gamma_{\max}}{2}\left(1 + k\,\frac{\sigma_{n,\max}}{S_y}\right) = \left[(1+\nu_e)\,\frac{\sigma_f'}{E}(2N_f)^b + (1+\nu_p)\,\varepsilon_f'\,(2N_f)^c\right] \times \left[1 + k\,\frac{\sigma_f'}{2S_y}(2N_f)^b\right] \tag{10.22}$$

where ν_e and ν_p are elastic and plastic Poisson ratios, respectively. Therefore, once the left side of Eq. 10.21 or Eq. 10.22 has been calculated for the multiaxial loading condition, fatigue life can be obtained. Equations 10.21 and 10.22 usually result in close agreement if shear fatigue properties and the value of k are available for the material. If these properties are estimated using the above approximations, discrepancies between lives predicted from the two equations can exist, as illustrated by the example problem in Section 10.4.3.

Figure 10.4 illustrates the correlation of multiaxial fatigue data for Inconel 718 using thin-walled tube specimens, based on the Fatemi-Socie parameter [10]. The data shown represent a wide variety of constant amplitude loading conditions obtained from in-phase (proportional) axial-torsion tests with or without mean stress, out-of-phase (nonproportional) axial-torsion tests, and biaxial tension tests (using internal/external pressurization) with or without mean stress. Park and Nelson [4] have evaluated this model for a variety of metallic alloys including mild steel, high-strength and high-temperature steel alloys, stainless steels, and several aluminum alloys under a wide variety of proportional and nonproportional constant amplitude loading conditions. The value of k for these materials ranged between 0 and 2. Good correlations of multiaxial fatigue lives are reported for the Fatemi-Socie model, as well as for the Park-Nelson energy-based model mentioned in Section 10.4.1.

According to the Fatemi-Socie model, cyclic shear strain must be present for fatigue damage to occur (Eq. 10.19 indicates no damage if $\Delta\gamma_{max}/2 = 0$). Therefore, this model is suitable for materials where the majority of the fatigue life is spent in crack nucleation and small crack growth along the maximum shear planes. This situation is representative of many metals and alloys. For some materials such as cast iron, however, crack nucleation and/or crack growth is along the maximum tensile stress or strain planes. In this case, the Smith-Watson-Topper parameter discussed in Section 5.6 can be used as the damage model, where the governing parameters are the maximum principal strain amplitude, ε_{a1}, and the maximum normal stress on the maximum principal strain amplitude plane, $\sigma_{n,max}$. The critical plane is then the plane with the largest value of $(\varepsilon_{a1}\sigma_{n,max})$. Similar to the Fatemi-Socie model, mean and residual stress effects and additional hardening due to nonproportional loading are incorporated through the maximum normal stress term.

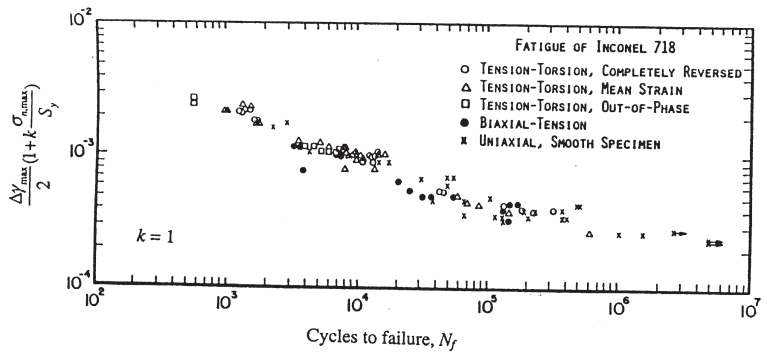

Figure 10.4 Correlation of Inconel 718 multiaxial fatigue data using the Fatemi-Socie parameter [10] (reprinted by permission of D. L. Morrow).

10.4.3 Example of Nonproportional Loading

Consider a smooth, thin-walled tube made of 1045 hot-rolled steel and subjected to cyclic 90° out-of-phase axial-torsion straining. Both axial and shear strains are fully reversed, with axial strain amplitude of $\varepsilon_{ax} = 0.0026$ and shear strain amplitude of $\gamma_{axy} = 0.0057$. We want to predict the fatigue life using the maximum shear strain theory and the Fatemi-Socie critical plane model.

The material has a yield strength of $S_y = 380$ MPa and the following strain–life properties [11]:

Torsion: $G = 80$ GPa, $\tau_f' = 505$ MPa, $b_0 = -0.097, \gamma_f' = 0.413, c_0 = -0.445$
Uniaxial: $E = 205$ GPa, $\sigma_f' = 948$ MPa, $b = -0.092$, $\varepsilon_f' = 0.26$, $c = -0.445$

The constant k in the Fatemi-Socie parameter for this material is 0.6, as found by fitting fully reversed uniaxial and torsional fatigue data.

The applied strain histories are given by the following equations:

$$\varepsilon_x = \varepsilon_{ax} \sin \omega t \quad \text{and} \quad \gamma_{xy} = \gamma_{axy} \sin (\omega t + 90°)$$

where the x axis is the tube's longitudinal axis. The applied strain path (γ_{xy}–ε_x plot), the resulting measured axial and torsional hysteresis loops, and the stress path (τ_{xy}–σ_x plot) are shown in Fig. 10.5 [12]. Variation of the applied strains (ε_x and γ_{xy}) and stable measured stresses (σ_x and τ_{xy}) during a cycle are shown in Fig. 10.6*a*. Note that due to the nonproportional nature of the loading, the hysteresis loops shown in Figs. 10.5*b* and 10.5*c* are rounded. As a result, there is a phase lag between the maximum values of axial strain and axial stress, and between the maximum values of shear strain and shear stress during a cycle, which can be observed in Fig. 10.6*a*.

To evaluate fatigue damage, it is important to realize that the maximum damage does not necessarily occur on the axial loading plane (i.e., x-plane). Instead, damage on different planes must be evaluated in order to determine the critical plane(s) with the maximum value of the damage parameter. Stress and strain transformation equations can be used to identify the critical plane(s). For example, shear strain on an arbitrary plane, γ_θ, is given by

$$\gamma_\theta = (\varepsilon_x - \varepsilon_y) \sin 2\theta - \gamma_{xy} \cos 2\theta$$

where θ is the angle between this arbitrary plane and the x-plane, ε_x and γ_{xy} are the applied strains, and ε_y is the transverse normal strain due to Poisson's effect calculated from

$$\varepsilon_y = -\nu\varepsilon_x = -[\nu_e\,(\varepsilon_x)_{\text{elastic}} + \nu_p\,(\varepsilon_x)_{\text{plastic}}] = -[0.3\,\sigma_x/E + 0.5(\varepsilon_x - \sigma_x/E)]$$
$$= 0.2\,\sigma_x/E - 0.5\,\varepsilon_x$$

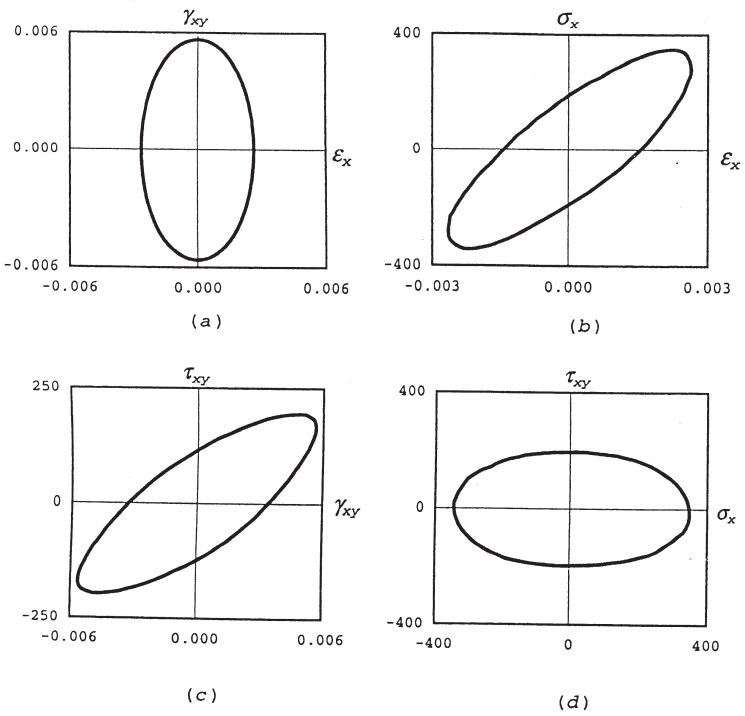

Figure 10.5 Deformation response from 90° out-of-phase axial-torsion straining [12]. (*a*) Applied strain path. (*b*) Stable axial hysteresis loop. (*c*) Stable torsion hysteresis loop. (*d*) Stress path (reprinted with permission of the Society of Automotive Engineers).

where elastic and plastic Poisson ratios are 0.3 and 0.5, respectively. Variation of the shear strain amplitude, $\Delta\gamma/2$, as a function of plane orientation angle, θ, is shown in Fig. 10.6*b*. As can be seen, the planes oriented at 0° and 90° (i.e., planes oriented perpendicular and parallel to the tube axis) are the planes experiencing the maximum shear strain range $\Delta\gamma_{max} = 0.0113$. The maximum shear strain amplitude can be related to the fatigue life in an analogous manner to the uniaxial strain–life relationship (Eq. 5.14), but with torsional strain–life properties as follows:

$$\frac{\Delta\gamma_{max}}{2} = \frac{\tau_f'}{G}(2N_f)^{b_0} + \gamma_f'(2N_f)^{c_0} = \frac{505}{80\,000}(2N_f)^{-0.097} + 0.413(2N_f)^{-0.445}$$

Substituting $\Delta\gamma_{max}/2 = 0.0057$ in this equation results in $N_f = 23\,000$ cycles.

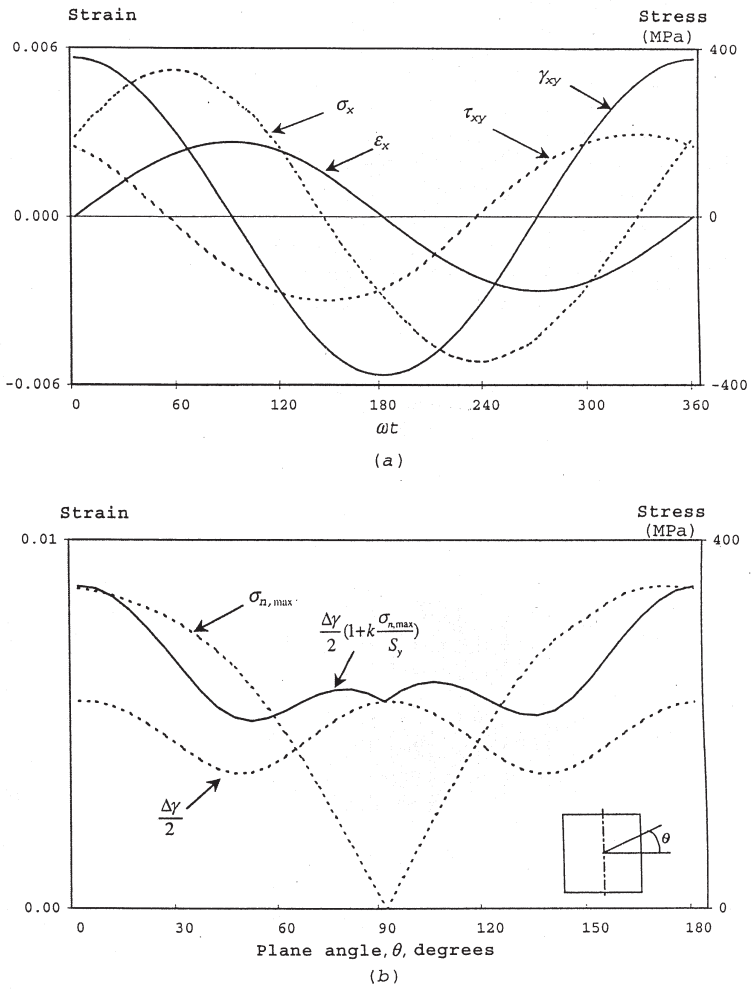

Figure 10.6 Stress and strain variations in a cycle and with plane orientation for 90° out-of-phase axial-torsion straining. (*a*) Stress and strain variations during one cycle. (*b*) Variation of shear strain range, maximum normal stress, and the Fatemi-Socie parameter with plane orientation.

To evaluate the Fatemi-Socie parameter, the normal stress on the maximum shear strain amplitude plane, $\sigma_{n,\max}$, must also be obtained. Variation of the normal stress as a function of plane orientation angle can be obtained by using the stress transformation equation and is shown in Fig. 10.6*b*. Spreadsheet calculations using digital computers are usually used to calculate different stress or strain quantities on different planes and at different times in the loading cycle. It can be seen that for this example, the maximum normal stress, $\sigma_{n,\max}$, occurs on the x-plane ($\theta = 0°$) with $\sigma_{n,\max} = 350$ MPa. Therefore, the critical plane is predicted to be the x-plane (perpendicular to the tube axis), since this plane experiences the largest values of both $\Delta\gamma$ and σ_n. Experimental results (i.e., cracking observations) for the material and loading in this example agree with this prediction [8]. Variation of the Fatemi-Socie parameter as a function of plane orientation angle is shown in Fig. 10.6*b*. To calculate fatigue life, Eq. 10.21 with the given values of k and S_y can be used:

$$\frac{\Delta\gamma_{\max}}{2}\left[1 + 0.6\,\frac{\sigma_{n,\max}}{380}\right] = \frac{505}{80\,000}\,(2N_f)^{-0.097} + 0.413\,(2N_f)^{-0.445}$$

Substituting $\Delta\gamma_{\max}/2 = 0.0057$ and $\sigma_{n,\max} = 350$ MPa from Fig. 10.6*b* in this equation results in $N_f = 6000$ cycles. Experimental life for the material and the loading condition described in this example problem was 5300 cycles [7], which is in close agreement with the prediction. If the fatigue properties from torsion tests and the value of k were not available, Eq. 10.22 with uniaxial fatigue properties could be used and the value of k can be approximated to be unity. In this case, the predicted life will be 9500 cycles, which is still reasonably close to the experimental life. The maximum shear strain theory overestimates the fatigue life (i.e., $N_f = 23\,000$ according to this theory), as it ignores the contribution of the normal stress to the damage process.

Average experimental fatigue life for in-phase (proportional) axial-torsion loading of the material in this example at the same strain amplitudes of $\varepsilon_{ax} = 0.0026$ and $\gamma_{axy} = 0.0057$ was observed to be 18 500 cycles [13]. This indicates a substantial reduction in fatigue life, down to 5300 cycles, as a result of applying the loads 90° out-of-phase. In general, fatigue life for in-phase versus out-of-phase loading can be compared based either on the magnitudes of the applied stress/strain amplitudes or on the magnitude of the maximum equivalent stress/strain amplitude. In other words, one method of comparing fatigue life can be based on the amplitudes of individual components of applied stress or strain, as was done in this example problem. A second method is to first combine the applied stress or strain components into an equivalent stress or strain and then use the amplitude of this equivalent stress or strain as the basis for comparison. If comparison is based on equal maximum equivalent stress/strain amplitude, out-of-phase loading is always equally or more damaging than in-phase loading. If comparison is based on equal applied stress/strain amplitudes, out-of-phase loading can be either less or more damaging than in-phase loading, depending on the material and its degree of additional cyclic hardening from out-of-phase loading. At high loads or in the low-cycle regime, where strains are mainly plastic, the additional cyclic hardening is higher that at lower loads or in the high-cycle regime, where strains are mainly elastic.

10.5 FRACTURE MECHANICS MODELS FOR FATIGUE CRACK GROWTH

Fracture mechanics is used to characterize the growth of cracks where multiaxial stress states can result in mixed-mode crack growth. A characteristic of mixed-mode fatigue cracks is that they can grow in a non-self similar manner, i.e., the crack changes its direction of growth. Therefore, under mixed-mode loading conditions, both crack growth direction and crack growth rate are important.

Different combinations of mixed-mode loading can exist from multiaxial loads. For example, in simple torsion of smooth shafts, surface cracks can form and grow in longitudinal and/or transverse directions along the maximum shear planes, where mixed-mode II and III exists along the crack front. Cracks can also form and grow along the ±45° angle to the axis of the shaft along planes of maximum principal stress where they grow in mode I. Plate components with edge or central cracks under in-plane biaxial tension or under three- or four-point bending and shear loading often produce mixed-mode I and II crack growth. In plate components, however, the mode I contribution often becomes dominant after a short period of crack growth.

Experimental observations suggest that the growth of cracks with small plastic zone size relative to the crack length depends mainly on the alternating stresses that pull the crack faces open (i.e., stresses normal to the crack plane). The other alternating stresses parallel to the crack do not often significantly affect the crack growth rate. However, if crack tip plasticity is large, stress components parallel to the crack can also significantly affect the crack growth rate.

Several parameters have been used to correlate fatigue crack growth rates under mixed-mode conditions. These include equivalent stress intensity factors, equivalent strain intensity factors, strain energy density, and the J-integral. For example, an equivalent stress intensity factor range, ΔK_q, based on crack tip displacements was proposed by Tanaka [14] and is given by

$$\Delta K_q = \left(\Delta K_{\mathrm{I}}^4 + 8\,\Delta K_{\mathrm{II}}^4 + \frac{8\,\Delta K_{\mathrm{III}}^4}{1-\nu}\right)^{0.25} \tag{10.23}$$

Another form of equivalent stress intensity factor is based on the equivalence of energy release rate, G, and the stress intensity factor, K, for nominal elastic

loading, as described in Chapter 6. Adding the individual energy release rates for a planar crack under plane stress conditions results in

$$G = G_{\mathrm{I}} + G_{\mathrm{II}} + G_{\mathrm{III}} = \frac{K_{\mathrm{I}}^2}{E} + \frac{K_{\mathrm{II}}^2}{E} + \frac{(1+\nu)\,K_{\mathrm{III}}^2}{E} \tag{10.24}$$

which leads to the following equivalent stress intensity factor range:

$$\Delta K_q = [\Delta K_{\mathrm{I}}^2 + \Delta K_{\mathrm{II}}^2 + (1+\nu)\,\Delta K_{\mathrm{III}}^2]^{0.5} \tag{10.25}$$

ΔK_q has been used for the mixed-mode loading condition in a Paris-type equation (Eq. 6.19) to obtain the crack growth rate, *da/dN,* or cycles to failure through integration.

In situations in which the plastic zone size is large compared to the crack length, such as in low-cycle fatigue or in growth of small cracks, equivalent strain intensity factors or the *J*-integral may be more suitable parameters to use. An equivalent strain intensity factor based on the Fatemi-Socie model (Eq. 10.19) has been shown to be successful in correlating small crack growth data from a variety of proportional and nonproportional axial-torsion tests with thin-walled tube specimens made of Inconel 718 and 1045 steels [15]. Detailed discussion of mixed-mode crack growth behavior can be found in [1,16].

10.6 NOTCH EFFECTS AND VARIABLE AMPLITUDE LOADING

Notches cannot be avoided in many components and structures. The severity of a notch is often characterized by the stress concentration factor, K_t. However, as discussed in Chapter 7, the stress concentration factor depends not only on the notch geometry, but also on the type of loading. It should also be recognized that the stress state at the root of the notch is often multiaxial even under uniaxial loading conditions. For example, in axial loading of a circumferentially notched bar, both axial and tangential stresses exist at the root of the notch. The tangential stress component results from the notch constraint in the transverse direction. In the *S–N* approach, fatigue strength can be divided by the fatigue notch factor, K_f. If the theoretical stress concentration factors, K_t's, for multiaxial loading differ too greatly for different principal directions, each nominal alternating stress component can be multiplied by its corresponding fatigue notch factor, K_f. This can be done because the *S–N* approach is used mainly for elastic behavior and, therefore, superposition can be used to estimate notch stresses from combined multiaxial loads. For example, for combined bending and torsion of a notched shaft and in the absence of mean stresses, an equivalent stress, based on the octahedral shear stress, can be computed as

$$S_{qa} = \sqrt{(K_{fB}\,S_B)^2 + 3\,(K_{fT}\,S_T)^2} \tag{10.26}$$

where S_B and S_T are nominal bending and torsion stresses, respectively, and K_{fB} and K_{fT} are fatigue notch factors in bending and torsion, respectively. Notch effects in the ε–*N* approach for multiaxial loading when notch root plastic deformation exists are more complex and often require the use of cyclic plasticity models. For this case, Neuber's rule is often generalized to the multiaxial loading situation by using equivalent stresses and strains. Detailed discussion of notch effects in the ε–*N* approach for multiaxial proportional and nonproportional stress states is provided in [1].

Multiaxial fatigue analysis for variable amplitude loading is quite complex, particularly when the applied loads are out-of-phase or nonproportional. Nevertheless, excellent axles and crankshafts subject to complex multiaxial fatigue are produced based on experience. Similar to uniaxial loading, the two main steps in cumulative damage analysis from multiaxial variable amplitude loading are identification or definition of a cycle and evaluation of damage for each identified or counted cycle. Several methods for predicting cumulative damage in multiaxial fatigue have been developed, such as those of Bannantine and Socie [17] and Wang and Brown [18]. Bannantine and Socie's method is based on the critical plane approach, in which cycles on various planes are counted and a search routine is then used to identify the plane experiencing the most damage (i.e., the critical plane). It should be noted, however, that the definition of the damage plane for the critical plane model used may not be unique during variable amplitude cyclic loading. For example, for the Fatemi-Socie critical plane model discussed in Section 10.4.2, the critical plane can be defined as either the maximum shear plane with the largest normal stress or the plane which experiences the maximum value of the damage parameter (i.e., the left side of Eq. 10.19). For constant amplitude proportional and nonproportional loading, the two definitions result in the same plane. This is illustrated in Fig. 10.6*b*, where the 0° plane is shown to have the maximum shear strain range, $\Delta\gamma_{\max}$, with the largest normal stress, $\sigma_{n,\max}$, as well as the maximum value of the damage parameter (shown by the solid curve). For complex variable amplitude loading, the two planes may be different. In this case, the plane having the largest value of the damage parameter should be chosen as the critical plane. Wang and Brown's method is based on counting cycles using an equivalent strain. Once cycles have been counted using one of the aforementioned methods, damage is accumulated for each cycle according to the Palmgren-Miner linear damage rule discussed in Chapter 9. Additional discussion of multiaxial variable ampltitude loading can be found in [1].

10.7 SUMMARY

Multiaxial states of stress are very common in engineering components and structures. Multiaxial cyclic loading can be categorized as proportional where

the orientation of the principal axes remains fixed or as nonproportional where the principal directions of the alternating stresses change orientation during cycling. Nonproportional cyclic loading involves greater difficulties and often produces additional cyclic hardening compared to proportional loading. Multiaxial fatigue analysis for situations in which significant plasticity exists often requires the use of a cyclic plasticity model consisting of a yield function, a flow rule, and a hardening rule.

Stress-based, strain-based, energy-based, and critical plane approaches have been used for life prediction under multiaxial stress states. The most common stress-based methods are those based on equivalent octahedral shear stress and the Sines method. Equivalent nominal stress amplitude based on the octahedral shear stress criterion and equivalent mean nominal stress based on hydrostatic stress are obtained from

$$S_{qa} = \frac{1}{\sqrt{2}}\sqrt{(S_{a1} - S_{a2})^2 + (S_{a2} - S_{a3})^2 + (S_{a3} - S_{a1})^2} \tag{10.9}$$

$$S_{qm} = S_{m1} + S_{m2} + S_{m3} \tag{10.11}$$

The S–N approach is limited primarily to elastic and proportional loading situations. Strain-based methods are based on equivalent strain. They may be suitable for inelastic loading, but their use is still limited to proportional loading conditions. Energy-based and critical plane approaches are more general approaches and are suitable for both proportional and nonproportional multiaxial loading. Critical plane approaches reflect the physical nature of fatigue damage and can predict both fatigue life and the orientation of the failure plane. A common critical plane approach is the Fatemi-Socie model:

$$\frac{\Delta\gamma_{\max}}{2}\left(1 + k\frac{\sigma_{n,\max}}{S_y}\right) = \frac{\tau_f'}{G}(2N_f)^{b_0} + \gamma_f'(2N_f)^{c_0} \tag{10.21}$$

Fracture mechanics models are used to characterize the growth of macrocracks in multiaxial fatigue, where mixed-mode crack growth often exists. Equivalent stress intensity factors have been used to relate mixed-mode crack growth data to mode I data from uniaxial loading. Notches and variable amplitude loading introduce additional complexities, particularly for nonproportional loading. Several methods to incorporate these effects have been developed.

10.8 DOS AND DON'TS IN DESIGN

1. Don't ignore the presence of multiaxial stress states, as they can significantly affect fatigue behavior. The state of stress at the root of a notch is usually multiaxial even under uniaxial loading conditions.

2. Do determine whether the alternating stresses or strains have fixed principal directions. If so, the loading is proportional and fairly simple methods for life estimation can be used.
3. Don't ignore the effects of nonproportional cyclic loading, since it can produce additional cyclic hardening and often results in a shorter fatigue life compared to proportional loading.
4. Do recognize that application of equivalent stress and equivalent strain approaches to multiaxial fatigue is limited to simple proportional or in-phase loading. Other methods such as the critical plane approach are more suitable for more complex nonproportional or out-of-phase loading.
5. Do determine whether the fatigue damage mechanism for the given material and loading is dominated by shear or by tensile cracking. Different fatigue damage models apply to each case.

REFERENCES

1. D. F. Socie and G. B. Marquis, *Multiaxial Fatigue,* Society of Automotive Engineers, Warrendale, PA, 1999.
2. G. Sines, "Behavior of Metals Under Complex Static and Alternating Stresses," *Metal Fatigue,* G. Sines and J. L. Waisman, eds., McGraw-Hill Book Co., New York, 1959, p. 145.
3. F. Ellyin, *Fatigue Damage, Crack Growth and Life Prediction,* Chapman and Hall, London, 1997.
4. J. Park and D. V. Nelson, "Evaluation of an Energy-Based Approach and a Critical Plane Approach for Predicting Multiaxial Fatigue Life," *Int. J. Fatigue,* Vol. 22, No. 1, 2000, p. 23.
5. W. N. Findley, "A Theory for the Effect for Mean Stress on Fatigue of Metals Under Combined Torsion and Axial Load or Bending," *Trans. ASME, J. Eng. Industry,* Vol. 81, 1959, p. 301.
6. M. W. Brown and K. J. Miller, "A Theory for Fatigue Under Multiaxial Stress–Strain Conditions," *Proceedings of the Institute of Mechanical Engineers,* Vol. 187, 1973, p. 745.
7. A. Fatemi and D. F. Socie, "A Critical Plane Approach to Multiaxial Fatigue Damage Including Out-of-Phase Loading," *Fatigue Fract. Eng. Mater. Struct.,* Vol. 11, No. 3, 1988, p. 149.
8. D. F. Socie, "Critical Plane Approaches for Multiaxial Fatigue Damage Assessment," *Advances in Multiaxial Fatigue,* ASTM STP 1191, D. L. McDowell and R. Ellis, eds., ASTM, West Conshohocken, PA, 1993, p. 7.
9. P. Kurath and A. Fatemi, "Cracking Mechanisms for Mean Stress/Strain Low-Cycle Multiaxial Loadings," *Quantitative Methods in Fractography,* ASTM STP 1085, B. M. Strauss and S. K. Putatunda, eds., ASTM, West Conshohocken, PA, 1990, p. 123.

10. D. L. Morrow, *Biaxial-Tension Fatigue of Inconel 718,* Ph.D. diss., University of Illinois, Urbana, 1988.
11. A. Fatemi and P. Kurath, "Multiaxial Fatigue Life Predictions Under the Influence of Mean Stresses," *Trans. ASME, J. Eng. Mater. Tech.,* Vol. 110, 1988, p. 380.
12. A. Fatemi and R. I. Stephens, "Cyclic Deformation of 1045 Steel Under In-Phase and 90 Deg Out-of-Phase Axial-Torsional Loading Conditions," *Multiaxial Fatigue: Analysis and Experiments,* SAE AE-14, G. E. Leese and D. F. Socie, eds., SAE, Warrendale, PA, 1989, p. 139.
13. A. Fatemi and R. I. Stephens, "Biaxial Fatigue of 1045 Steel Under In-Phase and 90 Deg Out-of-Phase Loading Conditions," *Multiaxial Fatigue: Analysis and Experiments,* SAE AE-14, G. E. Leese and D. F. Socie, eds., SAE, Warrendale, PA, 1989, p. 121.
14. K. Tanaka, "Fatigue Propagation from a Crack Inclined to the Cyclic Tensile Axis," *Eng. Fract. Mech.,* Vol. 6, 1974, p. 493.
15. S. C. Reddy and A. Fatemi, "Small Crack Growth in Multiaxial Fatigue," *Advances in Fatigue Lifetime Predictive Techniques,* ASTM STP 1122, M. R. Mitchell and R. W. Landgraf, eds., ASTM, West Conshohocken, PA, 1992, p. 276.
16. J. Qian and A. Fatemi, "Mixed Mode Fatigue Crack Growth: A Literature Survey," *Eng. Fract. Mech.,* Vol. 55, No. 6, 1996, p. 969.
17. J. A. Bannantine and D. F. Socie, "A Variable Amplitude Multiaxial Fatigue Life Prediction Method," *Fatigue Under Biaxial and Multiaxial Loading,* ESIS 10, Mechanical Engineering Publications, London, 1991, p. 35.
18. C. H. Wang and M. W. Brown, "Life Prediction Techniques for Variable Amplitude Multiaxial Fatigue—Part I: Theories," *Trans. ASME, J. Eng. Mater. Tech.* Vol. 118, 1996, p. 367.

PROBLEMS

1. Three common stress states are simple uniaxial tension, simple torsion, and equibiaxial tension. (*a*) Show the principal stress directions and the planes of maximum stress or strain and maximum shear stress or strain. (*b*) Plot the variation of the normal and shearing stresses as a function of plane orientation for the case of simple uniaxial tension.

2. An AISI 8640 steel shaft is Q&T to S_u = 1400 MPa (200 ksi) and S_y = 1250 MPa (180 ksi) with RA = 10 percent. A step with a fillet radius of 5 mm exists in the shaft that causes K_t = 2.1 in torsion. If the smaller shaft diameter is 50 mm, what maximum pulsating torque (R = 0) can be applied over a period of several years and last for at least 1 million cycles?

3. Repeat Problem 2 if the shaft is shot-peened, causing compressive residual stresses at the step equal to 700 MPa in both the longitudinal and transverse directions.

4. In Problems 2 and 3, what maximum torque can be applied for 50 000 cycles?

5. A 25 mm diameter 2024-T3 aluminum shaft is subject to constant amplitude in-phase bending and torsion. The bending moment varies from 0 to 144 N.m, and the torque varies from −100 to +200 N.m. (*a*) What is the safety factor against static yielding? (*b*) Will the shaft withstand 10 million cycles of this combined loading?

6. For Problem 5, how much could the bending moment be increased and still have a life of 50 000 cycles of combined loading?

7. Prove that the stress path for the 90° out-of-phase stressing in Fig. 10.1*d* is elliptical.

8. A smooth circular shaft is made of 1038 normalized steel and subject to completely reversed, constant amplitude torque. The torsion shear strain on the surface of the shaft is measured to be ±0.005. Determine the expected life according to (*a*) the maximum shear strain theory and (*b*) the octahedral shear strain theory.

9. Constant amplitude axial and torsion strain histories applied to a thin-walled tube are trapezoidal, as shown in part (*a*) of the following figure. (*a*) Plot the strain path (γ_{xy} versus ε_x) for this load history. (*b*) Is this proportional or nonproportional loading? (*c*) The tube is made of 1045 hot-rolled steel with properties given in Section 10.4.3 and the resulting stress response shown in part (*b*) of the figure. What is the expected fatigue life according to the maximum shear strain theory? (*d*) Repeat part (*c*) using the Fatemi-Socie critical plane model.